Oxo−Hydroxy Tautomerism of 5-Fluorouracil: Water-Assisted Proton Transfer

Nadezhda Markova, Venelin Enchev,* and Iliana Timtcheva

Institute of Organic Chemistry, Bulgarian Academy of Sciences, 1113 Sofia, Bulgaria

Received: August 26, 2004; In Final Form: December 11, 2004

Post-Hartree−Fock ab initio quantum chemical calculations were performed for 5-fluorouracil in the gas phase and in a three-water cluster. Full geometry optimizations of the 5-fluorouracil−water complexes were carried out at the MP2/6-31+G(d,p) level of theory. MP4/6-31+G(d,p)//MP2/6-31+G(d,p) and MP4/6-31++G-(d,p)//MP2/6-31+G(d,p) single-point calculations were performed to obtain more accurate energies. In water solution, 5-fluorouracil exists mainly in the 2,4-dioxo form (**A**). We propose that the populations of the 2-hydroxy-4-oxo (**B**) and 4-hydroxy-2-oxo (**D**) tautomers are 1×10^{-4}% and 3.9×10^{-8}%, respectively, on the basis of the relative stabilities of the tautomers calculated at the MP4/6-31++G(d,p)//MP2/6-31+G(d,p) level of theory. A profound difference between isolated and hydrated 5-fluorouracil is noted for the height of the tautomerization barrier. In the absence of water, the process of proton transfer is very slow. The addition of water molecules decreases the barrier by 2.3 times, making the process much faster. The minimum energy path (MP2/6-31+G(d,p)) for water-assisted proton transfer in trihydrated 5-fluorouracil was followed. CNDO/S-CI calculations predict singlet $\pi-\pi^*$ electron transitions at 312 nm for **B** and at 318 nm for **D**. The fluorescence spectrum of 5-fluorouracil in water confirms the presence of the hydroxy tautomer.

1. Introduction

The hypothesis of the occurrence of pyrimidine and purine bases in rare tautomeric forms has attracted considerable attention. In Löwdin's theory,[1] rare tautomeric forms of nucleic bases play an essential role in alteration of the normal base−base pairing, leading to transition-type point mutations. It has been suggested that 5-halogeno derivatives of uracil may occur in rare hydroxy forms.[2] For this reason, they can potentially act as mutagenic agents.

5-Fluorouracil (5FU) belongs to the pyrimidine bases and is a cytotoxic analogue of the natural base thymine that has proven useful in the chemotherapy of a number of cancers, particularly colorectal cancer. The incorporation of 5FU in place of thymidine in DNA may have other structural or functional ramifications that have not yet been explored.[3] 5FU is an antimetabolite drug and exerts its anticancer effects through the inhibition of thymidylate synthase and the incorporation of its metabolites into RNA and DNA.[4]

Experimental data[5−7] suggests that the dioxo-tautomer of 5FU is stable in the solid state, in nonwater solution, and in low-temperature matrices; rare tautomeric forms are not observed. Dobrowolski et al.[6] did not find in an argon matrix any traces of its rare tautomeric forms. In an attempt to predict accurate energy differences between the various tautomers of 5FU in the gas phase, numerous quantum chemical studies have been undertaken.[8−11] The stability difference relative to the other tautomers is large enough to guarantee that the dioxo tautomer is the only important tautomer in the gas phase and in solution, as suggested experimentally.[5−7]

The first ab initio investigation on 5-fluorouracil tautomerism in the gas phase was carried out by Scanlan and Hillier[8] at the HF/3-21G level of theory. Later, Les and Adamowicz[9] reported results for the three lowest-energy tautomers at the MP2 level of theory with the DZP basis set, but the optimized molecular structures and zero point energies (ZPEs) of the nuclear vibrational motions were obtained at the HF/3-21G level. In their opinion, the detection of the rare forms by spectroscopic methods was not possible. A possible exception might be UV fluorescence spectroscopy.

The solvent effect, especially of water, on the tautomeric equilibrium of 5-fluorouracil was studied by Russo et al.[10] and Yekeler and Özbakir[11] in the framework of the self-consistent reaction field (SCRF) model. Russo et al.[10] concluded that 5FU tautomers obey the stability sequence 2,4-dioxo > 2-hydroxy-4-oxo > 2-oxo-4-hydroxy > 2-hydroxy-4-hydroxy, and the presence of water does not affect the relative stabilities as found in the gas phase. However, it is known that the reaction field theory is appropriate only for solvents that do not give specific interactions, such as hydrogen bonding, with the solvent.

For the first time, H-bonding of 5-fluorouracil with water molecules was investigated at the HF/STO-3G level by Del Bene.[12] Recently, Dobrowolski et al.[5] reported theoretical and experimental ^{1}H, ^{13}C, ^{15}N, and ^{17}O NMR chemical shifts for the 2,4-dioxo tautomer of 5-halogenouracils. The solvent effect was estimated at the HF/3-21G(d,p) level by surrounding the 5-halogenouracil molecules with water molecules forming hydrogen bonds with electron donor and electron acceptor groups of the molecules. Using molecular dynamics (MD) and ab initio HF/6-31G(d) and DFT B3LYP/6-31G(d) methods, Ghio et al.[13] examined the interactions in aqueous solution for a variety of 5-fluorouracil dimers in water. In articles,[5,12,13] the calculations were performed for the 2,4-dioxo tautomer only.

Solute−solvent interactions not only determine the relative stability of the tautomeric forms but can also influence the interconversion mechanism. Protic solvents, like water, can accept a proton from the donor site of the solute molecule and transfer a different proton to the acceptor site on the solute. Water-assisted proton transfer mechanism studies have shown

* Correspondence to Venelin Enchev, Institute of Organic Chemistry, Bulgarian Academy of Sciences, 1113 Sofia, Bulgaria. E-mail: venelin@orgchm.bas.bg. Fax: ++359 2 8700225.

10.1021/jp046132m CCC: $30.25
Published on Web 02/15/2005

that the assistance of a water molecule significantly lowers the free energy barriers in proton-transfer-related reactions.[14−30] On the other hand, the electrostatic interaction of a solute molecule with a solvent represented by a continuum model only slightly influences the activation barriers of proton transfer reactions[31] (i.e., the influence of electrostatic interactions with the bulk is less important).

The solvent can control the dynamics of a proton transfer reaction via two distinct types of solute−solvent interactions. The first are long-range solvent polarization interactions, and the second are specific short-range hydrogen-bonding interactions. In the latter case, an explicit interaction with a limited number of solvent molecules could influence the whole reaction path by lowering the energy barrier due to the direct participation of solvent molecules in the proton transfer. The second case will be the subject of investigation in this paper.

2. Computational Details

It is well-known that the quantum chemical study of hydrogen-bonded systems requires the inclusion of dynamic correlation effects. Second-order Moller−Plesset perturbation theory has been proven to be an adequate choice. When the level of calculations is sufficiently high (e.g., MP2/6-31+G-(d,p)), the accuracy of the theoretical calculations can often exceed experimental results.[32]

Ab initio calculations using many-body perturbation theory (MBPT) were carried out in the study of the interaction of 5FU tautomers with three water molecules. All geometries of the minima and the transition structures for the tautomeric conversions were located at the MP2/6-31+G(d,p) level without symmetry restrictions, using the gradient procedure. The mean gradient threshold was 1×10^{-4} hartree b^{-1}. Frequency calculations at the same level of theory were carried out for all the complexes reported in the study to determine whether the optimized structures were local minima or transition states (TSs) on the potential energy surface and to estimate thermal corrections.

The values of Gibbs free energies and the corresponding equilibrium constants were calculated by the standard formulas $\Delta G = \Delta H - T\Delta S$ and $K = e^{-\Delta G/RT}$, respectively. To estimate ΔH values, thermal corrections to the enthalpies calculated at the MP2/6-31+G(d,p) level were added to the calculated energies. The entropy values were evaluated from the frequency calculations at the level of optimization. The classical rate constant at 298.15 K was calculated using the Eyring equation $k = (k_B T/h)\cdot\exp(-\Delta G^{\#}/RT)$, where k_B and h are the Boltzmann and Planck constants, respectively.

To establish the connection between transition structure and the corresponding equilibrium structures in the trihydrated complex of 5FU, the reaction pathway was followed using the intrinsic reaction coordinate (IRC) procedure. The fourth-order Runge−Kutta (RK4) algorithm[33,34] implemented in the *GAMESS* program package was used to obtain the IRC of the water-mediated proton transfer (PT) reaction. The reaction path was followed from the transition state to the reactant and to the product using a step size of 0.05 $amu^{1/2}$ b.

To obtain accurate energies, single-point calculations at MP4/6-31+G(d,p)//MP2/6-31+G(d,p) and MP4/6-31++G(d,p)//MP2/6-31+G(d,p) levels of theory were performed. The total energies were corrected for MP2/6-31+G(d,p) ZPEs. The unscaled ZPE corrections were included in the relative energy values.

All calculations were carried out using the PC *GAMESS* version of the *GAMESS* (U.S.A.) quantum chemistry package.[35]

To estimate the effect of the polar medium (water) on the relative stabilities of the tautomers of 5FU, we applied the polarizable continuum model (PCM)[36,37] as implemented in the *Gaussian 98*[38] suite of programs at the MP2/6-31+G(d,p) level for the geometries optimized at the same level of theory, PCM/MP2/6-31+G(d,p).

The energies of the electron transitions for some tautomers were calculated by means of the semiempirical CNDO/S-CI method[39] using the MP2/6-31+G(d,p) optimized geometries. All monoexcited configurations were included in the configuration interaction.

3. Experimental Section

5FU used in this study was purchased from Sigma, U.S.A.

Absorption spectra were scanned on a Specord M40 (Carl Zeiss, Jena) UV−vis spectrophotometer and the corrected fluorescence spectra on a Perkin-Elmer MPF44 spectrofluorimeter. The emission spectra were corrected using a standard tungsten lamp, while the excitation spectra were corrected with Rhodamine B. Deionized water was used as the solvent.

4. Results and Discussion

The main goal of this study is an evaluation of the water-assisted proton transfer in 5FU; thus, we are only interested in the hydrated forms of the compound. In such systems, the water molecules are specifically located in positions appropriate for direct assistance of the proton transfer process modifying the reaction path. The relative stabilities of isolated tautomeric forms of 5FU are considered only for comparison.

4.1. Relative Stabilities and Structures of Tautomers. The six possible tautomeric forms of 5FU and their rotamers are shown in Figure 1. All species were optimized at the HF/6-31+G(d,p) level of theory. The relative total energies of the dioxo, **A**, and different hydroxy tautomers, **B**−**F**, of 5FU in the gas phase are presented in Table 1. Selected structures were reoptimized at the MP2/6-31+G(d,p) level. The computed energies of the tautomers studied reveal that at the MP2/6-31+G(d,p) level of theory the 2,4-dioxo form, **A**, is the most stable, followed by the 2-hydroxy-4-oxo, **B**, the 2-hydroxy-4-hydroxy, **E**, and the 2-oxo-4-hydroxy, **D**, ones. Species **C** and **F** are more than 16 kcal mol^{-1} less stable than tautomer **A** and are not further considered in our analysis. If we compare the HF/6-31+G(d,p) and MP2/6-31+G(d,p) results, it can be concluded that the higher computational level decreases the energy difference between tautomers, but the stability sequence remains the same (Table 1).

We considered the effect of aqueous hydration using the supermolecule approach in which three water molecules are attached to the 5FU tautomers **A**, **B**, **D**, and **E**. We assume that water binding with 5FU is a three-hydrated complex in which two of the water molecules are bonded between the N−H and C=O groups, while the third water molecule is bonded between the C5−F and C6−H groups. The values of the relative energies obtained for three-hydrated complexes at the MP2/6-31+G(d,p) level are given in Table 1. As mentioned already, the stability sequence in the gas phase is **A** > **B** > **E** > **D**. Upon water complexation, the relative stabilities of the tautomers change: **A** > **B** > **D** > **E** (Table 1). While in the gas phase, tautomer **A** is 8.55 kcal/mol more stable than **B**; upon complexation with three water molecules, this value becomes 7.42 kcal mol^{-1}. For tautomer **D**, the change is more strongly expressed: 12.54 kcal mol^{-1} before and 8.92 kcal mol^{-1} after complexation. The energy difference between tautomers **A** and **E** almost does not change upon complexation (Table 1). The three-hydrated

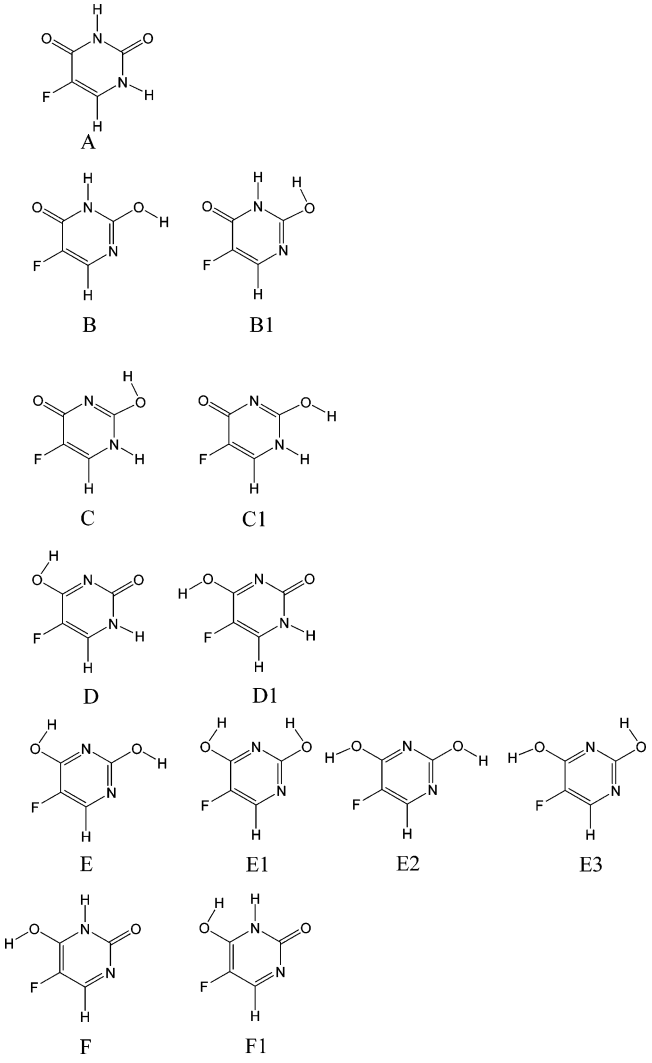

Figure 1. Tautomeric and rotameric forms of 5-fluorouracil.

complex of tautomer **E**, which is highest in energy and cannot be obtained directly from **A**, was not considered further. With the inclusion of ZPE corrections at the MP2/6-31+G(d,p) level, the tautomerization energy, ΔH_0, for the water complexes of **B** and **D** rises slightly: 7.55 and 9.08 kcal mol^{-1}, respectively. However, if the three-hydrated complexes of the 5FU tautomers are embedding in a continuum reaction field, tautomers **B** and **D** become almost equal in energy, with a small preference for **B** (Table 1).

To account for the possibility of the formation of intermolecular hydrogen bonding between tautomers **A**, **B**, and **D** of 5FU and water as the solvent, the interaction energies (E_{int}'s) for the trihydrated complex are considered:

$$E_{\text{int}} = E_{\text{5FU}} + 3E_{\text{water}} - E_{\text{complex}}$$

E_{5FU}, E_{complex}, and E_{water} are the E_{T} + ZPE energies, calculated at the MP2/6-31+G(d,p) level, for each 5FU tautomer, its trihydrated complex, and a water molecule, respectively. The values of E_{T} and the ZPE energies of the 5FU tautomers and their water complexes are presented in Table 1. The value of E_{water}, calculated at the same level of theory, is −76.211 469 au.

The calculated values of the interaction energies E_{int} of **A**, **B**, and **D** are 25.43, 26.14, and 28.48 kcal mol^{-1}, respectively. The water complex of **D** has the highest interaction energy, and thus, it is not surprising that in water solution the energy difference between tautomers **A** and **D** changes substantially in comparison with the that of the isolated molecules. The intermolecular hydrogen bonds O7···H12 and O16···H17 in the trihydrated complex of **A** (Figure 2) are longer than the same bonds in the trihydrated complex of **D** (Figure 3) by 0.078 and 0.003 Å, respectively, and the O8···H14 distance is longer than O13···H14 by 0.26 Å (Table 2).

The MP2/6-31+G(d,p)-optimized geometries of the trihydrated complexes of tautomers **A**, **B,** and **D** are presented in Figures 2 and 3. Selected interatomic distances are collected in Table 2. The obtained ab initio results for the geometry of tautomer **A** are in agreement with the X-ray data.[40]

As expected, the formation of a three-hydrated complex induces some changes in the geometrical parameters of **A**, **B**, and **D**, mainly in the region of intermolecular hydrogen bonding. According to calculations at the MP2/6-31+G(d,p) level for tautomer **A,** the changes in the carbonyl, N−H, and C−F bonds are strongest. The formation of an intermolecular hydrogen bond in the **A** + **3H$_2$O** complex leads to a lengthening of the C2═O7 and N3−H12 bonds by 0.011 Å and of the C6═O8 and N1−H11 bonds by 0.010 Å. The C5−F9 and C4−H9 bonds also lengthen by 0.009 and 0.001 Å, respectively, because of intermolecular hydrogen bonding. All single C−N and C−C bonds in the heterocycle ring shorten, while the double C4═C5 bond lengthens only by 0.002 Å. The shortening of the C5−C6 bond is more strongly expressed (0.010 Å) than that of the C−N bonds (0.007 Å) (Table 2). The effect of complexation is substantial for the water molecule, too. There is a lengthening (by 0.012 Å) of the O−H bond that participates in the intermolecular hydrogen bond (Figure 2).

The calculated vibrational spectrum of 5FU has been discussed by Blicharska and Kupka,[41] but the effect of H-bonding on the IR spectrum has not been considered. The geometry changes mentioned already are reflected in the calculated IR spectra of **A** and **A** + **3H$_2$O** (Table 3). The vibrational modes ν(N−H), ν(C═O), and γ(N−H) are highly affected by the presence of the surrounding water molecules. The N3−H and N1−H bond stretchings undergo strong wavenumber downshifts of 164 and 192 cm^{-1}, respectively, in going from isolated 5FU to the hydrated form, while the ν(C−H) and ν(C−F) modes are less affected by H-bonding. A remarkable increase in the intensity is observed in ν(N−H), indicating that hydration increases the polarizability of the N−H bond. The lengthening of the carbonyl bonds corresponds to the shift of the characteristic frequency to lower frequencies by 20 and 12 cm^{-1} for ν(C2═O) and ν(C6═O), respectively. The γ(N−H) vibrations are shifted to higher wavenumbers (25−50 cm^{-1}) upon hydration.

The MP2/6-31+G(d,p) calculated interatomic distances for the trihydrated complexes of hydroxy tautomers **B** and **D** are presented in Table 2. Changes are observed in the carbonyl and hydroxyl groups for both tautomers as a result of hydration. The C═O bond lengthens by 0.011 Å in the **B** + **3H$_2$O** complex and by 0.015 Å in **D** + **3H$_2$O**. Similarly, the O−H bond lengthens because of intermolecular hydrogen bonding, by 0.020 and 0.019 Å, respectively; the C−F bond by 0.010 and 0.006 Å. The C═N bond in the heterocyclic ring becomes longer by 0.013−0.014 Å, while the C4═C5 bond almost does not change upon hydration.

The values of the relative free energies ΔG's of the isolated tautomers shown in Table 1 suffer a very small variation on

TABLE 1: HF/6-31+G(d,p), MP2/6-31+G(d,p), and PCM/MP2/6-31+G(d,p) Calculated Total Energies (E_T's) and Zero-Point Energies (ZPEs) (a.u.) of 5-Fluorouracil Tautomers and their Trihydrated Complexes and Transition States[a]

	HF/6-31+G(d,p)		MP2/6-31+G(d,p)					PCM/MP2/6-31+G(d,p)		
species	E_T	ΔE_T	E_T	ZPE	ΔE_T	ΔH_0	ΔG	E_T	ΔE_T	ΔH_0
A	−511.331195	0.00	−512.699896	0.078755	0.00	0.00	0.00			
B	−511.315798	9.66	−512.686267	0.078237	8.55	8.23	8.41			
C	−511.303265	17.53	−512.673840	0.077645	16.35	15.65	15.52			
D	−511.308362	14.33	−512.679918	0.078057	12.54	12.10	12.06			
E	−511.312733	11.59	−512.684697	0.078387	9.53	9.31	9.69			
F	−511.294834	22.82	−512.666396	0.077308	21.02	20.11	19.89			
B1	−511.300658	19.16								
C1	−511.284416	29.35								
D1	−511.300472	19.28								
E1	−511.310659	12.89								
E2	−511.307681	14.76								
E3	−511.307570	14.82								
F1	−511.285476	28.69								
TS(A → B)			−512.626969	0.072927	45.76	42.11	42.00			
A + 3H$_2$O	−739.459114	0.00	−741.444350	0.152317	0.00	0.00	0.00	−741.463872	0.00	0.00
B + 3H$_2$O	−739.444363	9.26	−741.432528	0.152520	7.42	7.55	8.16	−741.450391	8.46	8.59
D + 3H$_2$O	−739.441104	11.30	−741.430128	0.152566	8.92	9.08	12.84	−741.450265	8.54	8.69
E + 3H$_2$O	−739.439426	12.35	−741.429414		9.37					
TS(A → B) + 3H$_2$O			−741.413307	0.146795	19.48	16.01	17.87	−741.431216	20.49	17.03
TS(A → D) + 3H$_2$O			−741.411879	0.146695	20.38	16.85	17.71	−741.431200	20.50	16.97

[a] Relative energies (ΔE_T), relative enthalpies at 0 K (ΔH_0), and relative Gibbs free energies (ΔG) are in kcal mol^{-1}.

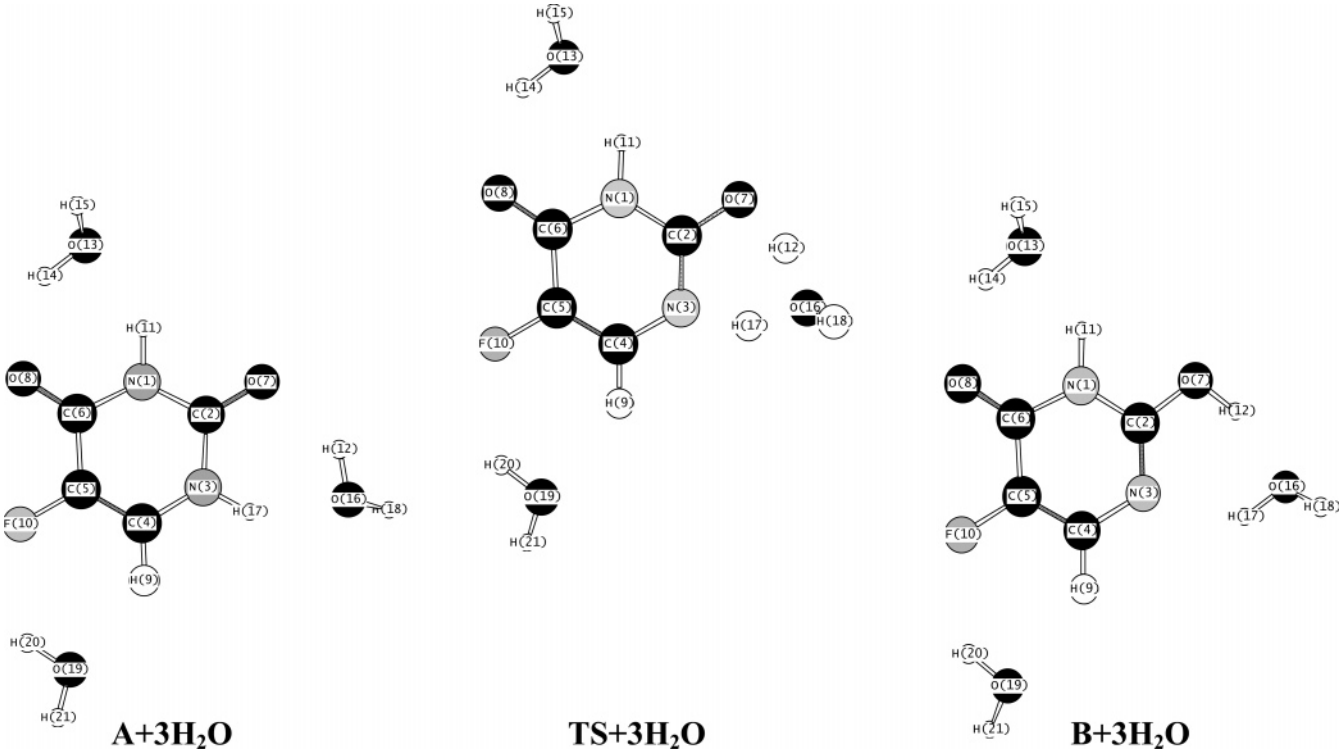

Figure 2. MP2/6-31+G(d,p)-optimized structures of the solvated tautomeric forms **A** and **B** and transition state **TS(A → B)**

account of the $T\Delta S$ term. More substantial changes are observed for hydrated tautomers **A**, **B**, and **D**: higher gaps between their stabilities. The equilibrium constants were calculated using the expression $K = e^{-\Delta G/RT}$. The values obtained for the hydrated forms are $K_{A\rightarrow B} = 1 \times 10^{-6}$ and $K_{A\rightarrow D} = 3.9 \times 10^{-10}$. These values suggest that the **B** and **D** tautomers fall in the range of the observed frequencies for spontaneous mutations ($10^{-8} - 1 \times 10^{-11}$).[11]

According to the relative stabilities calculated at the MP46-31++G(d,p)//MP2/6-31+G(d,p) level for species **A**, **B**, and **D**, the population of **D** is negligible, 3.9×10^{-8}%, because it is 11.50 kcal mol^{-1} higher in energy than **A** (Figure 4). However, a paltry fraction of enol form **B** cannot be ruled out, because this tautomer is 7.76 kcal mol^{-1} less favored than **A**, and the population of this tautomer in water solution is 1×10^{-4}%.

4.2. Proton Transfer. In this study, we consider the mechanism of tautomeric rearrangement in water solution of 5FU. The TS structures corresponding to the direct and assisted proton transfer reactions were found. The predicted TSs were verified by establishing that the Hessians have only one negative eigenvalue. The calculated barriers of the tautomerization reactions for the isolated (**A → B**) and trihydrated (**A → B** and **A → D**) 5FU and the respective imaginary frequencies, calculated at the MP2/6-31+G(d,p) level of theory, are presented in Table 4. The energy barriers were corrected for the ZPE obtained at the MP2/6-31+G(d,p) level of harmonic vibrational

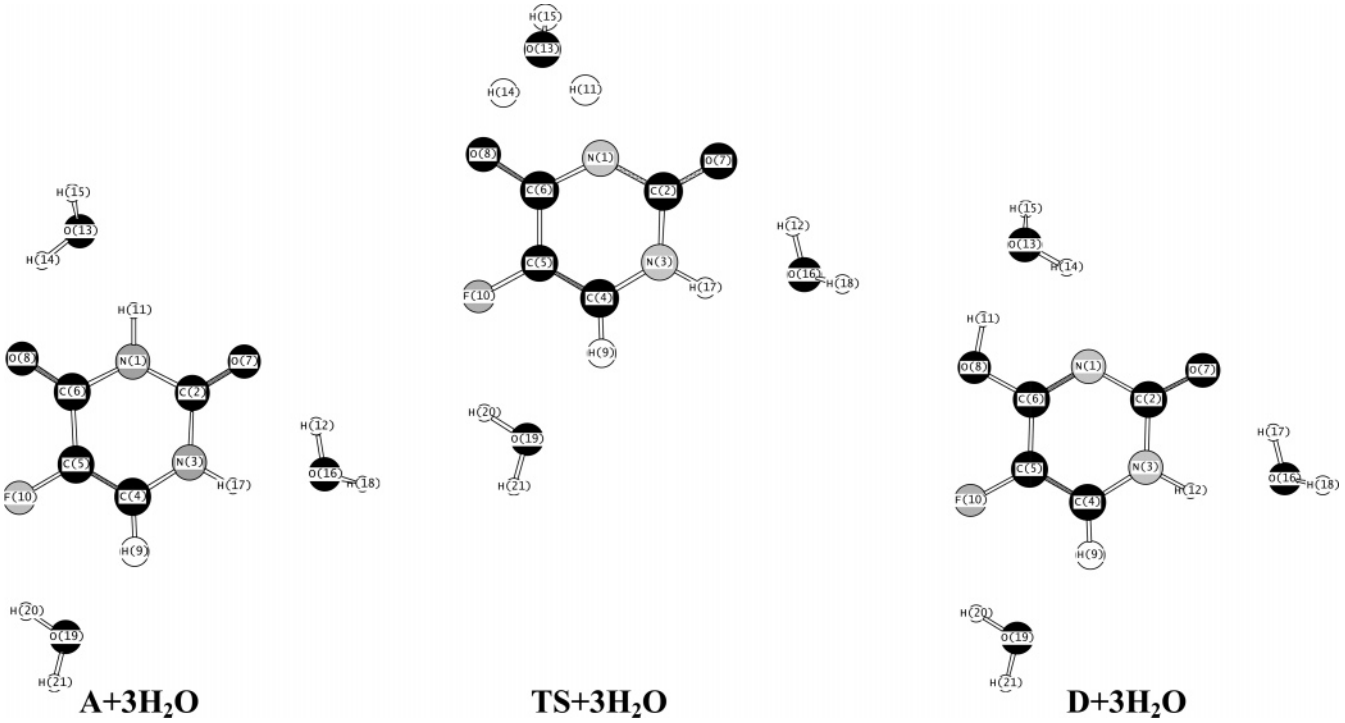

Figure 3. MP2/6-31+G(d,p)-optimized structures of the solvated tautomeric forms **A** and **D** and transition state **TS(A → D)**

TABLE 2: MP2/6-31+G(d,p) Calculated Interatomic Distances (Å) in Trihydrated Complexes of 5-Fluorouracil Tautomers A, B, D, and Respective Transition States[a]

distance	**A**		**B**	$\mathbf{TS_{A\rightarrow B}}$	**D**	$\mathbf{TS_{A\rightarrow D}}$
N1−C2	*1.392 (1.408)*	1.385	1.360	1.365	1.381	1.376
C2−O7	*1.227 (1.233)*	1.238	1.335	1.290	1.243	1.243
N3−C2	*1.386 (1.385)*	1.379	1.314	1.346	1.396	1.392
N3−H17	*1.010*	1.021	2.055	1.339	1.022	1.021
N3−C4	*1.383 (1.385)*	1.376	1.378	1.372	1.362	1.366
C4−H9	*1.080*	1.081	1.082	1.082	1.081	1.081
C4−C5	*1.350 (1.353)*	1.352	1.361	1.359	1.359	1.357
C5−F10	*1.350 (1.348)*	1.359	1.360	1.361	1.360	1.360
C5−C6	*1.461 (1.478)*	1.452	1.444	1.446	1.425	1.433
C6−O8	*1.228 (1.233)*	1.238	1.241	1.240	1.331	1.288
N1−C6	*1.404 (1.400)*	1.396	1.399	1.401	1.320	1.355
N1−H11	*1.014*	1.025	1.027	1.026	2.062	1.368
O7−H12		1.982	0.991	1.261	1.904	1.921
O16−H17		1.927	0.976	1.164	1.924	1.930
O16−H18		0.963	0.964	0.967	0.963	0.963
O16−H12		0.975	1.740	1.174	0.978	0.977
O19−H9		2.233	2.322	2.289	2.238	2.236
O19−H21		0.964	0.964	0.964	0.964	2.236
O19−H20		0.966	0.966	0.966	0.965	0.966
F10−H20		2.285	2.219	2.232	2.314	2.291
O13−H11		1.949	1.919	1.933	0.977	1.146
O13−H14		0.973	0.975	0.974	1.745	1.164
O13−H15		0.963	0.963	0.963	0.964	0.967
O8−H14		2.005	1.973	1.987	0.993	1.274

[a] Calculated data for isolated tautomer **A** are given in italics. Available X-ray data[40] are given in parentheses. For the numbering of the atoms, see Figures 2 and 3.

TABLE 3: Selected IR Data Calculated at MP2/6-31+G(d,p) Level for Isolated Tautomer A and Its Trihydrated Complex[a]

	isolated			hydrated
	exptl			
assigned[b]	ref 4	ref 42	calcd	calcd
ν(N3−H)	3480	3480	3484 (135)	3316 (494)
ν(N1−H)	3427	3416	3468 (83)	3276 (423)
ν(C4−H)			3109 (4)	3118 (45)
ν(C2═O) + δ(N1−H) + δ(N3−H)	1761	1754	1721 (778)	1701 (801)
ν(C6═O) + ν(C═C)	1742	1742	1687 (475)	1675 (459)
ν(C═C) + δ(C4−H)		1685	1636 (44)	1632 (50)
δ(N3−H) + ν(C4−N3)		1477	1443 (49)	1470 (18)
δ(N3−H) + ν(C−C) + ν(C2−N1)		1412	1371 (42)	1407 (34)
δ(N1−H) + δ(N3−H)		1386	1337 (3)	1385 (16)
δ(C4−H) + ν(C2−N1) + ν(C2−N3)		1334	1306 (34)	1322 (28)
ν (C−F) + ν(C4−N3)			1218 (192)	1219 (211)
δ(C4−H) + ν(C2−N1) + δ(N1−H)			1157 (161)	1193 (90)
δ(C4−H) + δ(N3−H) + ν(C4−N3)			1113 (23)	1138 (37)
ν(C2−N3) + δ(N1−H) + δ(CNC)			931 (14)	956 (10)
γ(C4−H)			813 (41)	865 (40)
ν(C−C)			708 (13)	722 (24)
γ(N3−C)			672 (5)	668 (3)
δ(C6═O)		539	589 (4)	604 (7)
γ(N3−H)			508 (36)	570 (194)
δ(ring)			429 (6)	439 (32)
δ(ring)			364 (19)	391 (51)
γ(ring)			303 (22)	314 (3)
δ(C−F) + δ(C═O)			284 (1)	310 (8)

[a] The frequencies, scaled by 0.945, are in cm^{-1}, and intensities (in brackets) are in km mol^{-1}. Available experimental data in argon matrix are given for comparison. [b] ν = stretching; δ = bending; γ = out-of-plane deformation.

frequency calculations. The TS geometries corresponding to water-assisted proton transfer in the trihydrated complexes **A** → **B** and **A** → **D** are shown in Figures 2 and 3, respectively.

The potential energy of the three-hydrated 5FU−water complex along the minimum energy path, calculated at the MP2/6-31+G(d,p) level, is illustrated in Figure 5. Reaction **A** → **B** has a lower barrier than **A** → **D** does. Upon examination of the structural changes from reactant to product in the **A** → **B** reaction, it can be concluded that the N3−C2−O7 bond angle is compressed by 2.3° from the equilibrium value and the N3−H17 bond is stretched from an equilibrium value of 1.021 Å to 1.339 Å at the transition state. Simultaneously, the O16−H12 bond lengthens from 0.975 Å in the equilibrium structure to 1.174 Å at the transition state. Similar changes are observed for the **A** → **D** reaction.

We define the forward reaction as the proton transfer from the dioxo form to the hydroxy forms of 5FU and its hydrated complexes, and we define the reverse as the reaction in the

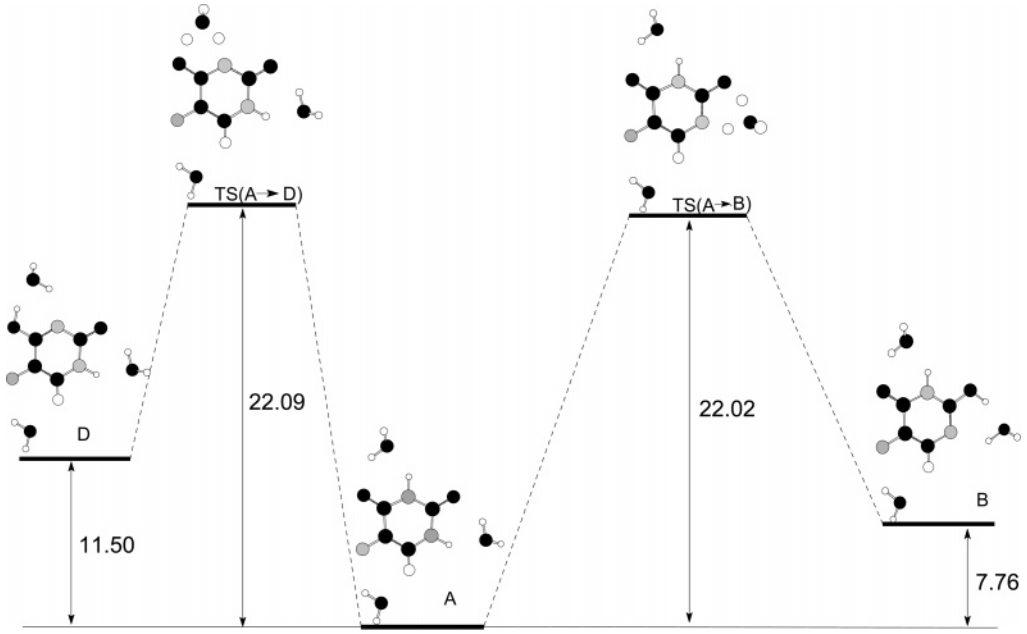

Figure 4. Energy profile of the tautomerization reactions **D** ← **A** → **B**, calculated at the MP4/6-31++G(d,p)//MP2/6-31+G(d,p) level. The relative activation free energies and activation barriers are given in kcal mol^{-1}.

TABLE 4: Calculated Energy Barriers $\Delta H_0^{\#}$ and $\Delta G_{298}^{\#}$ (in kcal mol^{-1}) for 5-Fluorouracil and Its Water Complexes Shown in Figures 2 and 3[a]

	reaction											
	A → B				A + 3H$_2$O → B + 3H$_2$O				A + 3H$_2$O → D + 3H$_2$O			
computational level	ΔH_0	ΔG_{298}	k	$\nu^{\#}$	ΔH_0	ΔG_{298}	k	$\nu^{\#}$	ΔH_0	ΔG_{298}	k	$\nu^{\#}$
MP2/6-31+G(d,p)	42.11	42.00	1.0×10^{-21}	1892*i*	16.01	17.87	4.9×10^{-4}	1496*i*	16.85	17.71	6.5×10^{-4}	1439*i*
MP4/6-31+G(d,p)//MP2/6-31+G(d,p)	45.81	45.34	3.6×10^{-24}		20.25	22.11	3.8×10^{-7}		21.24	22.09	4.0×10^{-7}	
MP4/6-31++G(d,p)//MP2/6-31+G(d,p)	45.24	44.76	9.6×10^{-24}		20.16	22.02	4.5×10^{-7}		21.23	22.09	4.0×10^{-7}	

[a] Imaginary frequencies $\nu^{\#}$'s are in cm^{-1}. Rate constants are in s^{-1}.

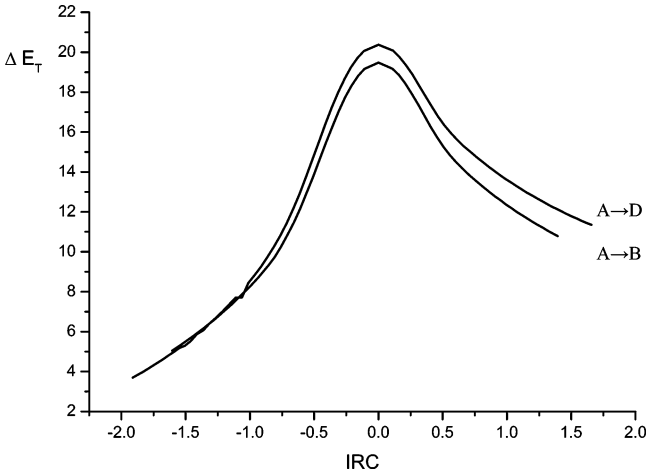

Figure 5. MP2/6-31+G(d,p)-calculated IRC profiles of the solvent-mediated proton transfer reactions in the 5-fluorouracil−water complexes **A** → **B** (Figure 2) and **A** → **D** (Figure 3). ΔE_T is in kcal mol^{-1} and IRC in amu$^{1/2}$ bohr.

opposite direction. The calculated values of the proton transfer barriers in 5FU and its water complexes are collected in Table 4. The activation energy of tautomerization reaction **A** → **B** via direct intramolecular proton transfer is very high, and the tautomerization process should not occur: the rate constant is on the order of 10^{-21}−10^{-24} depending on the level of calculation. The inclusion of water molecules dramatically reduces the activation energy. For the trihydrated complex, the proton transfer activation energy for the same reaction is lower than that for the isolated molecule by 22.7−24.3 kcal mol^{-1} at different computational levels. Because of the high sensitivity of the barrier height to the employed level of electron correlation,[19,30] the observed difference between MP4 and MP2 results is not surprising.

If we consider the three-hydrated complexes of the 5FU as embedded in a continuum reaction field, the energy barriers of reactions **A** → **B** and **A** → **D**, calculated at the MP2/6-31+G-(d,p) level, increase by 1.02 and 0.12 kcal mol^{-1}, respectively (Table 1).

At 0 K (i.e., $\Delta H_0^{\#}$), the energy barrier of the assisted proton transfer **A** → **B** reaction is lower than that of the **A** → **D** one. The situation changes if the $T\Delta S^{\#}$ term is taken into account. A plot of the resulting activation barrier dependencies on the temperature is shown in Figure 6. The activation energies are independent of temperature in the range 0−60 K. As can be seen in Figure 6, the computed activation barriers for processes **A** → **B** and **A** → **D** become the same at approximately 260 K at the MP2/6-31+G(d,p)//MP2/6-31+G(d,p) level and at 298 K at the MP4/6-31+G(d,p)//MP2/6-31+G(d,p) level. It can be seen that there exists the possibility for two parallel reactions **D** ← **A** → **B,** because both barriers are close in energy (Table 4 and Figure 6). The MP4/6-31++G(d,p)//MP2/6-31+G(d,p)-calculated activation barriers for reactions **A** → **B** and **A** → **D** at 298.15 K are shown in Figure 4.

Simple transition-state theory was applied to estimate the rate constants k's of the concurrent processes **A** → **B** and **A** → **D** using the Eyring equation. The computed classical rate constants k's of the proton transfer in 5FU are listed in Table 4. Because

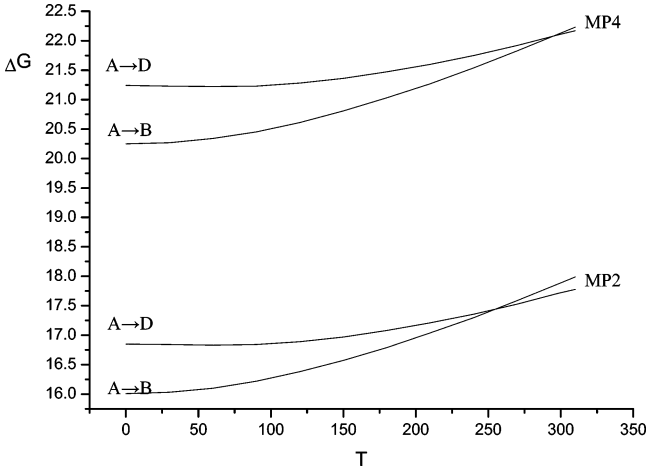

Figure 6. Plot of activation barriers (kcal mol^{-1}) vs temperature (K) for reactions **A** → **B** and **A** → **D** shown in Figure 4, calculated at the MP4/6-31+G(d,p)//MP2/6-31+G(d,p) and MP2/6-31+G(d,p) levels.

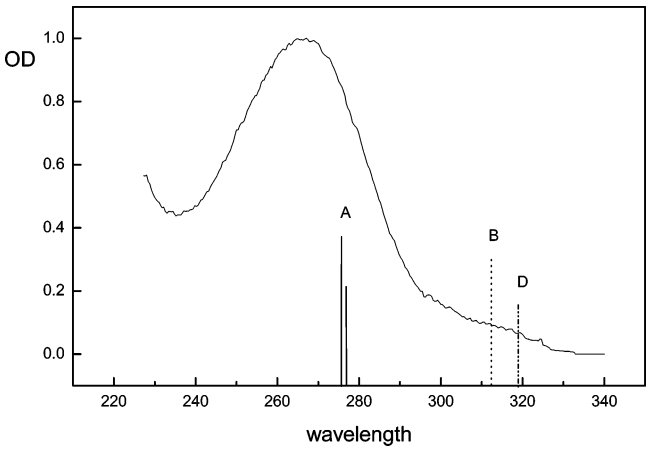

Figure 7. UV absorption spectrum of 5FU in water. Optical density (OD) is in arbitrary units and wavelength in nanometers. CNDO/S-CI-calculated $\pi-\pi^*$ electron transitions for tautomer **A** (solid line), tautomer **B** (dot line), and tautomer **D** (dash-dot-dot line).

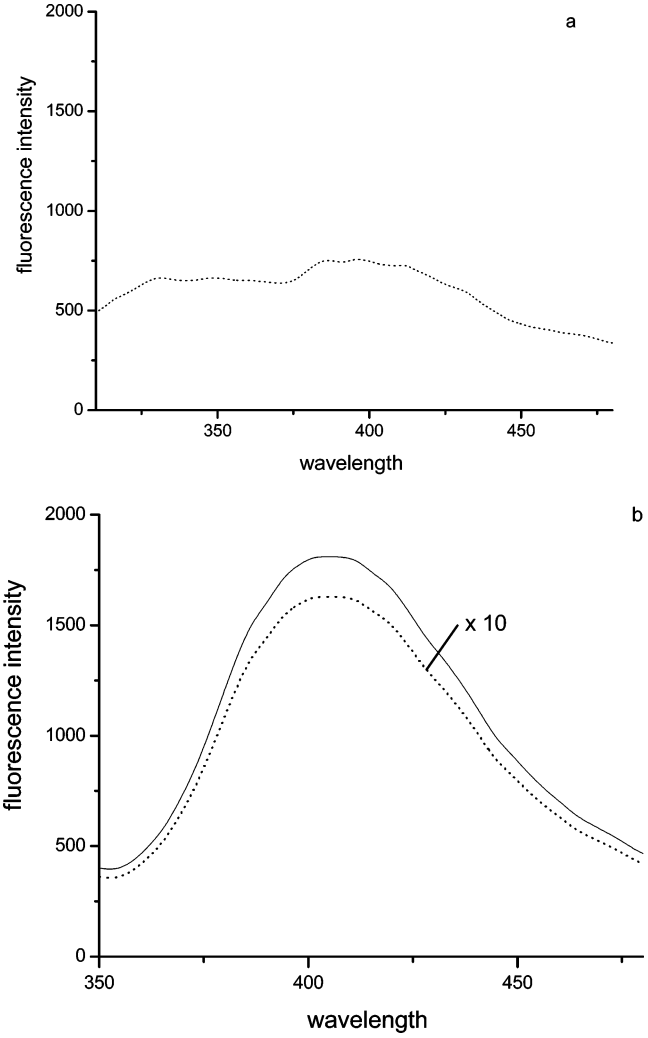

Figure 8. Fluorescence spectra of 5FU in deionized water (concentration of 5×10^{-5} mol L^{-1}). Fluorescence intensity is in arbitrary units, and wavelength is in nanometers. (a) Fluorescence spectrum of the starting solution, $\lambda_{exc} = 270$ nm. (b) (Dot line) fluorescence spectrum of the starting solution, $\lambda_{exc} = 310$ nm; (solid line) fluorescence spectrum of the same solution kept 10 days in dark, $\lambda_{exc} = 310$ nm.

of the exponential dependence of the rate constants on $\Delta G^{\#}$, their values differ by 3 orders of magnitude for the different levels of calculations. According to the rate constant values obtained at all levels of calculation, the forward assisted proton-transfer reaction can occur ($k_{\text{assisted PT}} = 10^{-4}-10^{-7} \gg k_{\text{direct PT}} = 10^{-21}-10^{-24}$), although slowly. This suggests that the forward reaction rate constant is more of a limiting factor than the equilibrium constant. Therefore, the forward reaction rate constant is large enough to be able to generate a concentration of rare tautomeric forms significant enough to reproduce the frequency of point mutations.

4.3. UV and Fluorescence Spectra. CNDO/S-CI calculations were performed to predict the absorption maxima of tautomers **A**, **B**, and **D**. For tautomer **A**, absorption maxima were calculated at 277 and 275 nm. The computed vertical singlet transition energies were found to be in good agreement with the corresponding experimental data (Figure 7). For tautomer **B**, an absorption maximum was predicted at 318 nm and for tautomer **D** at 312 nm. (Figure 7). The calculated electron spectra of the hydroxy tautomers **B** and **D** display a similarity with respect to their transition energies as well as their transition types. This is to be expected, because the molecular structures of these tautomers are similar.

To confirm the formation of hydroxy tautomers, the changes in the fluorescence spectrum of 5FU in deionized water were followed in time. The fluorescence spectrum of 5FU immediately after dissolving in deionized water upon excitation at 270 nm has two maxima with very low intensities at around 330 and 410 nm (Figure 8a). The first one is characteristic for 5FU, while the second one is most probably due to the fluorescence of the hydroxy tautomers. When the excitation wavelength is fixed at 310 nm, where the absorption maximum (Figure 7) of hydroxy tautomers is expected to be according to the quantum chemical calculations, the fluorescence maximum at 410 nm is also observed. The changes in the emission spectrum of this solution kept in the dark for 1, 2, 5, and 10 days were followed. After 10 days, the fluorescence maximum at 410 nm has approximately a 10-fold higher intensity than that of the starting solution (Figure 8b). This experimental result indicates that the concentration of the formed hydroxy tautomers increases with time.

Suwaiyan et al.[2,43] have performed detailed spectroscopic studies in aqueous solution of 5-chlorouracil[2] and thymine[43] at room temperature and have suggested the existence of a small amount of the hydroxy tautomer. These authors have found that the fluorescence band for an aqueous solution of the dioxo tautomer of thymine lies near 325 nm when excited in the range 260−270 nm. A much stronger broad fluorescence band with

a peak near 405 nm has been observed with the excitation of the sample at 295 nm. These experimental findings correspond to our results.

5. Conclusions

This study devoted to water-assisted proton transfer in 5-fluorouracil reveals a picture that differs from the gas-phase results. We predict at the MP4/6-31++G(d,p)//MP2/6-31+G-(d,p) level of theory that 5FU should exist in three forms: mainly 2,4-dioxo, and 1×10^{-4}% of the 2-hydroxy-4-oxo and 3.9×10^{-8}% of the 4-hydroxy-2-oxo form.

Hydration has an appreciable effect on the structure of the transition states corresponding to proton transfer from the 2,4-dioxo to the hydroxy tautomeric forms of 5FU. There is a dramatic decrease in the barrier heights when a water molecule participates directly in the proton transfer reaction. The values of proton transfer barriers decrease 2.0−2.3 times for the forward reaction, and the values of the rate constants increase by up to 17 orders of magnitude, at the MP46-31++G(d,p)//MP2/6-31+G(d,p) level of theory. The calculated barriers for the water-assisted proton transfer reactions **A** → **B** and **A** → **D** predicted in this study indicate that the tautomeric conversions from **A** to **B** and **A** to **D** are kinetically feasible processes and might play a key role in mutagenic events.

The CNDO/S-CI calculations predict $\pi-\pi^*$ electron transitions at 312 and 318 nm for the rare tautomeric forms **B** and **D**, respectively. The fluorescence spectroscopic study of 5FU in aqueous medium confirms the presence of hydroxy tautomeric forms.

References and Notes

(1) Löwdin, P.-O. *Rev. Mod. Phys*. **1963**, *35*, 724−732.
(2) Suwaiyan, A.; Morsy, M. A.; Odah, K. A. *Chem. Phys. Lett*. **1995**, *237*, 349−355.
(3) Kremer, A. B.; Mikita, T.; Beardsley, G. P. *Biochemistry* **1987**, *26*, 391−397.
(4) Longley, D. B.; Harkin, D. P.; Johnston, P. G. *Nat. Rev. Cancer* **2003**, *3*, 330−338
(5) Bednarek, E.; Dobrowolski, J. C.; Dobrosz-Teperek, K.; Kozerski, L.; Lewandowski, W.; Mazurek, A. P. *J. Mol. Struct*. **2000,** *554*, 233−243.
(6) Zwierzchowska, Z.; Dobrosz-Teperek, K.; Lewandowski, W.; Kolos, R.; Bajdor, K.; Dobrowolski, J. C.; Mazurek, A. P. *J. Mol. Struct*. **1997,** *410*−*411*, 415−420.
(7) Dobrosz-Teperek, K.; Zwierzchowska, Z.; Lewandowski, W.; Bajdor, K.; Dobrowolski, J. C.; Mazurek, A. P. *J. Mol. Struct*. **1998**, *471*, 115−121.
(8) Scanlan, M. J.; Hillier, I. H. *J. Am. Chem. Soc*. **1984,** *106*, 3737−3745.
(9) Les, A.; Adamowicz, L. *J. Phys. Chem*. **1989**, *93*, 7078−7081.
(10) Marino, T.; Russo, N.; Toscano, M. *Int. J. Quantum Chem*. **1997**, *62*, 489−494.
(11) Yekeler, H.; Özbakir, D. *J. Mol. Model*. **2001**, *7*, 103−111.
(12) Del Bene, J. E. *J. Phys. Chem*. **1982,** *86*, 1341−1347.
(13) Alagona, G.; Ghio, C.; Monti, S. *Int. J. Quantum Chem*. **2002**, *88*, 133−146.
(14) Wang, X.-C.; Nichols, J.; Feyereisen, M.; Gutowski, M.; Boatz, J. A.; Haymet, A. D.; Simons, J. *J. Phys. Chem*. **1991**, *95*, 10419−10424.
(15) Adamo, C.; Barone, V. *Properties and Chemistry of Biomolecular Systems*; Russo, N., Anastassopoulou, J., Barone, G., Eds.; Kluwer: Amsterdam 1994, 1−18.
(16) Gordon, M. S. *J. Phys. Chem*. **1996**, *100*, 3974−3979.
(17) Barone, V.; Adamo, C. *Int. J. Quantum Chem*. **1997,** *61*, 429−441.
(18) Adamo, C.; Cossi, M.; Barone, V. *J. Comput. Chem*. **1997**, *18*, 1993−2000.
(19) Bell, R. L.; Taveras, D. L.; Truong, T. N.; Simons, J. *Int. J. Quantum Chem*. **1997**, *63*, 861−874.
(20) Gorb, L.; Leszczynski, J. *J. Am. Chem. Soc*. **1998**, *120*, 5024−5032.
(21) Gu, J.; Leszczynski, J. *J. Phys. Chem. A* **1999**, *103*, 577−584.
(22) Chaban, G. M.; Gordon, M. S. *J. Phys. Chem. A* **1999**, *103*, 185−189.
(23) Zhanpeisov, N. U.; Cox, W. W., Jr.; Leszczynsky, J. *J. Phys. Chem. A* **1999**, *103*, 4564−4571.
(24) Shukla, M. K.; Leszczynski, J. *J. Phys. Chem. A* **2000**, *104*, 3021−3027.
(25) Shukla, M. K.; Leszczynski, J. *THEOCHEM* **2000**, *529*, 99−112.
(26) Gorb, L.; Podolyan, Y.; Leszczynski, J.; Siebrand, W.; Fernandez-Ramos, A.; Smedarchina, Z. *Biopolymers* **2001**, *61*, 77−83.
(27) Gorb, L.; Podolyan, Y.; Blue, A.; Leszczynski, J. *THEOCHEM* **2001**, *549*, 101−109.
(28) Podolyan, Y.; Gorb, L.; Leszczynski, J. *Int. J. Mol. Sci.* **2003**, *4*, 410−421.
(29) Balta, B.; Aviyente, V. *J. Comput. Chem*. **2004**, *25*, 690−703.
(30) Markova, N.; Enchev, V. *THEOCHEM* **2004**, *679*, 195−205.
(31) Antonczak, S.; Ruiz-López, M. F.; Rivail, J. L. *J. Am. Chem. Soc.* **1994**, *116*, 3912−3921.
(32) Elguero, J.; Katritzky, A. R.; Denisko, O. V. *Adv. Heterocycl. Chem.* **2000,** *76*, 1−84.
(33) Schmidt, M. W.; Gordon, M. S.; Dupuis, M. *J. Am. Chem. Soc*. **1985**, *107*, 2585−2589.
(34) Baldridge, K. K.; Gordon, M. S.; Steckler, R.; Truhlar, D. G. *J. Phys. Chem.* **1989**, *93*, 5107−5119.
(35) Schmidt, M. W.; Baldridge, K. K.; Boatz, J. A.; Elbert, S. T.; Gordon, M. S.; Jensen, J. H.; Koseki, S.; Matsunaga, N.; Nguyen, K. A.; Su, S.; Windus, T. L.; Dupuis, M.; Montgomery, J. A. *J. Comput. Chem.* **1993**, *14*, 1347−1363.
(36) Miertus, S.; Scrocco, E.; Tomasi, J. *Chem. Phys.* **1981**, *55*, 117−129.
(37) Miertus, S.; Tomasi, J. *Chem. Phys* **1982**, *65*, 239−245.
(38) Frisch, M. J.; Trucks, G. W.; Schlegel, H. B.; Scuseria, G. E.; Robb, M. A.; Cheeseman, J. R.; Zakrzewski, V. G.; Montgomery, J. A., Jr.; Stratmann, R. E.; Burant, J. C.; Dapprich, S.; Millam, J. M.; Daniels, A. D.; Kudin, K. N.; Strain, M. C.; Farkas, O.; Tomasi, J.; Barone, V.; Cossi, M.; Cammi, R.; Mennucci, B.; Pomelli, C.; Adamo, C.; Clifford, S.; Ochterski, J.; Petersson, G. A.; Ayala, P. Y.; Cui, Q.; Morokuma, K.; Malick, D. K.; Rabuck, A. D.; Raghavachari, K.; Foresman, J. B.; Cioslowski, J.; Ortiz, J. V.; Stefanov, B. B.; Liu, G.; Liashenko, A.; Piskorz, P.; Komaromi, I.; Gomperts, R.; Martin, R. L.; Fox, D. J.; Keith, T.; Al-Laham, M. A.; Peng, C. Y.; Nanayakkara, A.; Gonzalez, C.; Challacombe, M.; Gill, P. M. W.; Johnson, B. G.; Chen, W.; Wong, M. W.; Andres, J. L.; Head-Gordon, M.; Replogle, E. S.; Pople, J. A. *Gaussian 98*, revision A.7; Gaussian, Inc.: Pittsburgh, PA, 1998.
(39) Del Bene, J.; Jaffe, H. *J. Chem. Phys.* **1968**, *48*, 1807−1813.
(40) Fallon, L., III *Acta Crystallogr., Sect. B* **1973**, *29*, 2549−2556.
(41) Blicharska, B.; Kupka, T. *J. Mol. Struct.* **2002**, *613*, 153−166.
(42) Graindourze, M.; Grootaers, T.; Smets, J.; Zeegers-Huyskens, Th.; Maes, G. *J. Mol. Struct.* **1990**, *237*, 389−410.
(43) Morsy, M. A.; Al-Somali, A. M.; Suwaiyan, A. *J. Phys. Chem. B* **1999**, *103*, 11205−11210.